Published in final edited form as:
Dev Biol. 2011 December 1; 360(1): 66–76. doi:10.1016/j.ydbio.2011.09.001.

Mutations in Traf3ip1 reveal defects in ciliogenesis, embryonic development, and altered cell size regulation

Nicolas F. Berbari[a], **Nicholas W. Kin**[b], **Neeraj Sharma**[a], **Edward J. Michaud**[c], **Robert A. Kesterson**[d], and **Bradley K. Yoder**[a,*]

[a]Department of Cell Biology, University of Alabama at Birmingham, Birmingham, AL 35294 USA

[b]Department of Microbiology, University of Alabama at Birmingham, Birmingham, AL 35294 USA

[c]School of Physician Assistant Studies, South College, Knoxville, Tennessee 37909

[d]Department of Genetics, University of Alabama at Birmingham, Birmingham, AL 35294 USA

Abstract

Tumor necrosis factor alpha receptor 3 interacting protein 1 (Traf3ip1), also known as MIPT3, was initially characterized through its interactions with tubulin, actin, TNFR-associated factor-3 (Traf3), IL-13R1, and DISC1. It functions as an inhibitor of IL-13-mediated phosphorylation of Stat6 and in sequestration of Traf3 and DISC1 to the cytoskeleton. Studies of the Traf3ip1 homologs in *C. elegans* (DYF-11), Zebrafish (elipsa), and *Chlamydomonas* (IFT54) revealed that the protein localizes to the cilium and is required for ciliogenesis. Similar localization data has now been reported for mammalian Traf3ip1. This raises the possibility that Traf3ip1 has an evolutionarily conserved role in mammalian ciliogenesis in addition to its previously indicated functions. To evaluate this possibility, a Traf3ip1 mutant mouse line was generated. Traf3ip1mutant cells are unable to form cilia. Homozygous Traf3ip1 mutant mice are not viable and have both neural developmental defects and polydactyly, phenotypes typical of mouse mutants with ciliary assembly defects. Furthermore, in Traf3ip1 mutants the hedgehog pathway is disrupted, as evidenced by abnormal dorsal-ventral neural tube patterning and diminished expression of a hedgehog reporter. Analysis of the canonical Wnt pathway indicates that it was largely unaffected; however, specific domains in the pharyngeal arches have elevated levels of reporter activity. Interestingly, Traf3ip1 mutant embryos and cells failed to show alterations in IL-13 signaling, one of the pathways associated with its initial discovery. Novel phenotypes observed in Traf3ip1 mutant cells include elevated cytosolic levels of acetylated microtubules and a marked increase in cell size in culture. The enlarged Traf3ip1 mutant cell size was associated with elevated basal mTor pathway activity. Taken together, these data demonstrate that Traf3ip1 function is highly conserved in ciliogenesis and is important for proper regulation of a number of essential developmental and cellular pathways. The Traf3ip1 mutant mouse and cell lines will

*Corresponding Author: Bradley K. Yoder, Ph.D., Department of Cell Biology, 1918 University Blvd., Birmingham, AL 35294, Phone: (205) 934-0995, FAX: (205) 934-0990, byoder@uab.edu.

provide valuable resources to assess cilia function in mammalian development and also serve as a tool to explore the potential connections between cilia and cytoskeletal dynamics, mTor regulation, and cell volume control.

Keywords

primary cilia; IFT; Traf3ip1; MIPT3

Introduction

Primary cilia are solitary immotile appendages found on nearly all mammalian cell types where they serve important sensory and signaling roles essential for normal development and adult homeostasis (for a recent review see (Berbari et al., 2009)). The cilium is assembled through an evolutionarily conserved process called intraflagellar transport (IFT). IFT mediates the bi-directional movement of proteins between the base and tip of the cilium and is vital for transport of both structural and signaling components of the cilium. Numerous proteins are required for assembly of the IFT particle; for example interaction with kinesin and dynein motor proteins is crucial for the loading and unloading of cargo destined for delivery to and from the ciliary compartment. Relatively little is known about how the IFT particle is assembled or regulated in mammalian systems, although genetic and biochemical studies in model systems such as *C. elegans* and *Chlamydomonas* are providing important insights (for a review on IFT see (Pedersen and Rosenbaum, 2008)).

Defects in cilia structure or function are associated with multiple human genetic disorders collectively termed ciliopathies. These disorders exhibit a wide range of clinical features including anosmia, retinopathy, mental retardation, infertility, obesity, cystic kidney disease, *situs inversus*, and polydactyly (Sharma et al., 2008). While the molecular mechanisms contributing to these clinical features remain poorly defined, it is thought that the breadth of affected tissues and organ systems is due to the presence of primary cilia on most mammalian cell types as well as ciliary involvement in undetermined signaling pathways. Furthermore, cilia contain distinct complements of signaling machinery depending on the specific cell types on which they are found, suggesting that not all cilia are created equal in their signaling capabilities (Berbari et al., 2009). Although human ciliopathy patients offer excellent opportunities to study primary cilia functions, these patients are relatively rare and only a few of the mutations involve *bona fide* IFT genes (Arts et al., 2011; Cavalcanti et al., 2011). Thus, most insights into the molecular functions of cilia and IFT proteins in humans have been derived from comparative phenotypic analyses of genetic models across diverse systems.

There are several signaling pathways such as hedgehog (Hh) and wingless (Wnt) that have been associated with the cilium. Mutations in IFT genes or other ciliary proteins result in aberrant regulation of these pathways. For example, cilia regulate both activator and repressor functions of the Gli proteins in the Hh pathway. As such, in the absence of the cilium, the entire pathway becomes deregulated (Houde et al., 2006, Haycraft,2005#172; Huangfu et al., 2003; Liu et al., 2005). Cilia also appear to be important for noncanonical

Wnt-mediated suppression of the canonical Wnt pathway, although involvement of cilia in the latter has recently been questioned (Gerdes and Katsanis, 2008b; Ocbina et al., 2009). The cilium has also been implicated as a mechanosensor, detecting fluid-flow mediated shear stress across cells in the renal tubule and endothelium and possibly in bone and chondrocytes (Haycraft et al., 2007; Nauli et al., 2003; Nauli et al., 2008). In addition, the cilium is required for photoreception in the retina and for chemosensation in olfaction. Some of the disease phenotypes (e.g. retinal degeneration, anosmia, cerebellar hypoplasia, polydactyly) observed in human ciliopathy patients can be explained by defects in the aforementioned pathways (for a review on ciliopathies see (Sharma et al., 2008)). However, many have not been associated with defects in any particular pathway. These data suggest that the cilium is involved in additional signaling activities that have yet to be determined.

Intriguingly, a protein recently reported to be essential for ciliogenesis in *C. elegans* (dyf-11), Zebrafish (elipsa), and *Chlamydomonas* (IFT54) was identified in mammalian systems as tumor necrosis factor alpha receptor 3 interacting protein 1 (Traf3ip1)/ microtubule interacting protein that associates with Traf3 (MIP-T3, hereinafter called Traf3ip1) (Kunitomo and Iino, 2008; Li et al., 2008). In contrast to the ciliary/IFT role for the homologs in lower model organisms, in mammals Traf3ip1 is reported to bind with IL-13Rα1 and functions to repress IL-13 signaling by impairing IL-13 induced STAT6 phosphorylation (Niu et al., 2003). Traf3ip1 has also been shown to regulate functions of protein such as Traf3 and DISC1 by sequestration of these factors to microtubules (Niu et al., 2003). In the case of Traf3, ligand stimulation of cytokine receptors, such as CD40, causes the dissociation of the Traf3-MIP-T3 and recruitment of Traf3 to the CD40 receptor (Ling and Goeddel, 2000). Further, Traf3ip1 was found to bind both actin and tubulin, leading to the speculation that it is involved in regulating cytoskeletal dynamics (Guo et al., 2010). More recent data have indicated that Traf3ip also localizes to the cilium in mammalian cell lines (Follit et al., 2009); however, the importance of this localization and its association with the aforementioned functions is not known. Together, these data raise the possibility that Traf3ip1 is a multifunctional protein that has an evolutionarily conserved role as a component of the IFT system as well as additional roles in regulating pathways, such as IL-13 and CD40, that have not previously been associated with the cilium.

Methods and materials

Generation of Traf3ip1 Gene Trap Allele Mice

The Traf3ip1 mutant line (Traf3ip1$^{Gt(RRJ005)Byg}$, BayGenomics, San Francisco, CA; hereinafter called Traf3ip1^{GT}) was generated using embryonic stem cells in which a β-galactosidase neomycin resistance fusion cassette inserted into intron 11 of Traf3ip1. The insertion site was confirmed by genomic PCR and sequence analysis. PCR primers for genotyping were designed based on the insertion site (sequences available upon request). The embryonic stem cells containing the gene trap were on the 129P2/OlaHsd background and were injected into C57BL/6 blastocysts using standard procedures. Chimeras were then crossed with albino C57BL/6 females and germline transmission was confirmed by coat color and subsequent PCR genotyping. After observing no homozygous mutant offspring, timed pregnancies for embryo analysis were performed. Wildtype and Traf3ip1 embryos

were generated by intercrossing heterozygous animals and harvested at the indicated embryonic days with the morning of vaginal plug being embryonic day 0.5 (E0.5).

Quantitative Real Time PCR Analysis

Quantitative real-time (qRT) PCR analysis of RNA isolated from mouse embryonic fibroblasts was performed using iQ SYBR Green Supermix (Bio-Rad, Hercules, CA, USA) with the CFX96 real-timePCR detection system (Bio-Rad) as previously reported (Croyle et al., 2011). The primers for qRT-PCR analysis were generated in the 3 prime end of the Traf3ip1 transcript after the gene trap insertion (sequences available upon request).

Wnt and Hh Reporter Mice Analysis

The activity of the canonical Wnt pathway was analyzed by crossing compound heterozygous reporter [BAT-gal (Tg(BAT-lacZ)3Picc)(Maretto et al., 2003) or Ptch-Lacz ((Ptch1^{tm1Mps})(Goodrich et al., 1997))]; Traf3ip1^{GT} males with Traf3ip1^{GT} heterozygous females. Embryos from timed pregnancies were dissected at E10.5 and reporter gene activity in embryos was detected as previously described (Maretto et al., 2003).

Mouse Embryonic Fibroblast Generation

Mouse embryonic fibroblasts (MEFs) were harvested from E9.5 embryos and cultured in DMEM growth medium with High Glucose, 0.05mg/ml Penicillin/Streptomycin, 2mM L-Glutamine, 0.2mM β-mercaptoethanol, and 10% Fetal Bovine Serum (FBS). Prior to immunolabeling, MEFs were cultured in reduced serum medium containing 0.5% FBS for 48 hours to induce primary cilia formation.

Expression Plasmid Construction

The coding sequence of Traf3ip1 was amplified using Gateway-compatible primers from reverse-transcribed mouse whole-brain RNA generated using the Superscript First-Strand Synthesis RT-PCR Kit (Invitrogen, Carlsbad, CA). PCR amplification was performed with Phusion Taq Polymerase (New England Biolabs, Ipswich, MA). All DNA constructs were sequence verified (primer sequences are available upon request).

Cell Culture and Transient Transfections

IMCD-3 cells (ATCC, Manassas, VA) were maintained in DMEM:F12 medium supplemented with 10% FBS, 1.2 g/L of sodium bicarbonate, and 0.5 mM sodium pyruvate. 5×10^6 cells were electroporated with 10 μg of DNA and plated at high density on glass coverslips as previously described (Berbari et al., 2008). Cells were fixed 24–48 hours post-transfection for immunocytochemistry. MEFs were treated with mouse recombinant IL-13 (10ng/mL) from eBioscience for 20 minutes prior to protein isolation.

Immunoblotting

Cells were scraped into ice-cold lysis buffer (137 mM NaCl, 20 mM Tris pH 8.0, 1% Triton X-100, 10% glycerol, and complete EDTA-free protease inhibitor cocktail (Roche Diagnostics, Indianapolis, IN)). Cells were disrupted by passage several times through a syringe attached to a 30.5 gauge needle. The lysates were incubated on ice for 30 minutes

and vortexed. Protein concentrations were determined by the Bradford assay (Bio-Rad Laboratories, Hercules, CA). Protein samples were resolved on a denaturing 10% Tris-HCL gel (Bio-Rad Laboratories, Hercules, CA) and transferred to Immobilon-Psq transfer membrane (Millipore, Billerica, MA). Membranes were blocked in TBS-T (10mM Tris-HCl pH 7.5, 150 mM NaCl, 0.1% Tween-20) with 5% milk for 1 hour and incubated with primary antibody diluted in TBS-T with 2% BSA for 16–24 hours at 4 C. Membranes were probed with horseradish peroxidase (HRP) conjugated secondary antibodies diluted in TBS-T with 1% milk for 1 hour at room temperature. Secondary antibodies were detected using SuperSignal West Pico Chemiluminescent Substrate (Pierce, Waltham, MA) and bands were visualized using Blue Ultra Autorad Film (Bioexpress ISC). The following primary antibodies and dilutions were used: anti-S6 (#2317) 1:1000, anti-p-S6 Ser240/244 (#2215) 1:1000, anti-p-S6 Ser235/236 (#2211) 1:1000, anti-p70S6K, (#9202) 1:1000, anti-p-p70S6K (#9205) 1:1000, anti-STAT6 (#9362) 1:1000, anti-pSTAT6 (#9361) 1:1000 (Cell Signaling, Beverly, MA), anti-acetylated α-tubulin (T7451) anti-gamma tubulin (T6557) (Sigma, St. Louis, MO) 1:1000, anti-GM130 (gift from Dr. Elizabeth Sztul) 1:1000 and anti-α-tubulin (ab18251 Abcam, Cambridgeshire, UK) 1:1000. Secondary antibodies were HRP conjugated anti-rabbit (#31460) 1:5000, HRP conjugated anti-mouse (#31430) 1:10000 (Pierce/Thermo Scientific, Waltham, MA). Band density was determined using the ImageJ software (NIH).

Flow Cytometry

Single cell suspensions of MEF cultures were generated by trypsin treatment to release the cells followed by a media wash with 20% FBS to quench the tryptic digestion. Cells were then centrifuged and resuspended in PBS with 2% FBS. Cells were gated on total live cells (Propidium Iodide negative) and relative forward scatter (FSC) was determined. All flow cytometry analyses were performed on a FACSCalibur (BD Biosciences, Franklin Lakes, NJ) and analyzed using FlowJo software (Tree Star, Ashland, OR).

Immunofluorescence

Cells were fixed in 4% paraformaldehyde and permeabilized with 0.3% Triton X-100 in PBS with 2% donkey serum, 0.02% sodium azide and 10 mg/ml bovine serum albumin (BSA). Cells were labeled with anti-acetylated α-tubulin, 1:1000 (T-6793; Sigma-Aldrich, St. Louis, MO), anti-Arl13b, 1:1000 (gift of Dr. Tamara Caspary, Emory University), anti-IFT20, 1:500 (gift of Dr. Greg Pazour, University of Massachusetts) and the following antibodies from Developmental Studies Hybridoma Bank (University of Iowa, Iowa City, IA): anti-ShhN (5E1), anti-Nkx6.1, 1:100 (F65A2), anti-Mnr2, 1:100 (81.5C10), and anti-Msx1+2, 1:100 (4G1). All incubations and washes were carried out in PBS with 2% normal donkey serum, 0.02% sodium azide and 10 mg/ml BSA. Primary antibody incubations were performed for 16–24 hours at 4°C and secondary antibody incubations were performed for 1 hour at room temperature. Secondary antibodies included: Alexa Fluor-546 conjugated donkey anti-mouse IgG (Invitrogen, Carlsbad, CA), and Alexa Fluor 488-conjugated donkey anti-goat IgG (Invitrogen, Carlsbad, CA). Nuclei were visualized by Hoescht nuclear stain (Invitrogen, Carlsbad, CA). Coverslips were mounted using Immu-Mount (Fisher Scientific, Pittsburgh, PA).

Confocal Microscopy

All fluorescence images were captured on Perkin Elmer ERS 6FE spinning disk confocal microscope and images were processed and analyzed in Volocity version 5.3 software (Perkin Elmer, Shelton, CT).

Results

To assess Traf3ip1 subcellular localization and to explore conserved function, we expressed Traf3ip1 as a GFP fusion in mouse inner-medullary renal collecting duct cells (IMCD3). Localization of Traf3ip1-GFP was observed in both the cilia axoneme (Figure 1A inset) as well as at the basal body (Figure 1A–F), consistent with previous reports (Follit et al., 2009; Li et al., 2008). Cytosolic GFP localization was also evident, which may be an artifact of overexpression of the GFP fusion protein based on the data from a recent study of the endogenously expressed Traf3ip1 using affinity purified antiserum (Kunitomo and Iino, 2008).

To explore the possible roles of Traf3ip1, as well as its putative conserved function as an IFT protein, a Traf3ip1 mutant mouse line was created using an embryonic stem cell line harboring a gene trap (Traf3ip1^{GT}) insertion in intron 11 of Traf3ip1 (Figure 2A). From more than ten Traf3ip1^{GT} heterozygous intercrosses yielding more than 100 offspring no viable Traf3ip1^{GT} homozygous mutant mice were obtained indicating that loss of Traf3ip1 function is lethal. Furthermore, real-time quantitative PCR analysis (qRT) in Traf3ip1^{GT} mouse embryonic fibroblasts (MEFs) showed near 90% reduction in transcript levels (Figure 2B) compared to wildtype MEFs. Analysis of embryos from timed pregnancies indicated homozygous Traf3ip1^{GT} mutants are embryonic lethal with none developing past E13.5. However, near-Mendelian ratios were observed at E10.5 (23 wildtype; 66 Traf3ip1^{GT} heterozygotes; 22 Traf3ip1^{GT} homozygotes). This variability may be due to the remaining low-level expression of Traf3ip1 in the gene trap allele or influences of the genetic background (129/Ola and C57BL/6).

Analysis of the mutant embryos revealed several phenotypes commonly associated with cilia abnormalities including neural developmental defects (Figure 2C, D, G), cardiac edema (Figure 2E), and polydactyly (Figure 2F). Microphthalmia was also observed in several mutant embryos (Figure 2D arrow). Taken together, these data show that the Traf3ip1^{GT} allele causes embryonic lethality and results in a greater than 90% loss of Traf3ip1 mRNA. This suggests that this gene trap allele does disrupt most of the Traf3ip1 function and in general the phenotypes agree with those reported in other IFT and cilia mutant mice.

Data from multiple lower eukaryotic systems suggest that Traf3ip1 is essential for cilia formation (Li et al., 2008). To directly test the hypothesis that Traf3ip1 plays an evolutionarily conserved role in ciliogenesis, Traf3ip1^{GT} homozygous mutant cells and embryos were immunolabeled with cilia markers. Labeling of serum-starved, primary mouse embryonic fibroblasts (MEF) from Traf3ip1^{GT} and control mice with acetylated α-tubulin (Figure 3A, B) and sections from E10.5 embryos with the cilia marker Arl13b (Figure 3E, F) indicated that the mutants have a marked reduction in the number of cilia both *in vitro* and *in vivo*.

In previous studies, it was shown that overexpression of Traf3ip1 in mammalian cells caused displacement of IFT20 from the Golgi (Follit et al., 2009). Thus, we analyzed whether loss of Traf3ip1 may also alter IFT20; however, immunofluorescence analysis showed no significant differences in IFT20 localization (Supplemental Figure 1*A, B*) (Follit et al., 2009). Taken together, the localization of Traf3ip1 protein (Figure 1), the mutant phenotype (Figure 2), and the absence of cilia on mutant cells (Figure 3) indicate that Traf3ip1 plays a conserved role in mammalian ciliogenesis.

A striking observation made in Traf3ip1^{GT} mutant cells was the substantial increase in the levels of cytosolic acetylated α-tubulin in cell lines (Figure 3 and Supplemental Figure 1). These effects were observed in multiple independent embryonic fibroblast lines isolated from the Traf3ip1 mutants. To further assess the cause of the increase in acetylated α-tubulin, protein lysates were isolated from the MEFs and analyzed by western blot. The data indicated that there were no changes in total tubulin levels but rather an overall increase in acetylation (Figure 3C and D) when compared to GAPDH. To determine if similar effects occurred *in vivo*, sections of E10.5 mutant embryo were immunolabeled with anti-acetylated α-tubulin. Interestingly, this phenotype was only observed in certain regions of the embryo. For example, in the lateral plate mesenchyme, which is ciliated at this time (Figure 3E and F), there did not appear to be higher levels of acetylated α-tubulin staining by immunofluorescence; however, in the neural tube of Traf3ip1^{GT} mutants there was an increase in acetylated α-tubulin when compared to Traf3ip1^{WT} sections (Figure 3G and H). Although the cause of the increased acetylation is unknown, the data indicate that loss of cilia may enhance cytosolic microtubule stability or increase the activity or microtubule access to an acetyl-transferase.

In addition to increased microtubule acetylation, embryonic fibroblasts from Traf3ip1^{GT} mutants were significantly larger as determined by confocal fluorescence microscopy and flow cytometry (Figure 3B and D). In contrast to the microtubule acetylation data, this effect appears to be observed only under *in vitro* conditions. The cause of the discrepancy between the *in vitro* and *in vivo* data is currently unknown. Cell size control is a complex process involving the integration of nutrient status and growth factors in the cells' environment. In part, cell volume is regulated through the mammalian target of rapamycin (mTor) pathway. Furthermore, recent data have demonstrated a link between cilia dysfunction in cystic kidney disease mouse and cell culture models and regulation of mTorC1 activity that subsequently influences cell size (Boehlke et al., 2010; Bonnet et al., 2009; Hartman et al., 2009). To further investigate this connection, we compared the mTor pathway activity in the Traf3ip1^{GT} mutant and control cells both *in vivo* and *in vitro*. In the absence of serum Traf3ip1^{GT} mutant and wildtype MEFs showed basal levels of phospho-mTor (p-mTor) and had similar low levels of phospho-p70S6 kinase (p-p70 S6K), the direct downstream target of mTor (Figure 4A and Supplemental Figure 2*A*). Both mutant and control MEFs showed a response to pathway activation after only 5 minutes of serum treatment (Figure 4A and B) which was still seen after 1.5 and 3 hour treatment (Supplemental Figure 2*B*). Serum induced activation of the mTor pathway could be equally impaired in control and mutant cells by addition of rapamycin (Supplemental Figure 2*A*). Quantification of the data from multiple experiments indicates that the extent of the activation was generally more dramatic

and prolonged in the Traf3ip1^{GT} mutants compared to the control MEF cells. This is shown by the elevated levels of phosphorylated mTor, p70 S6 kinase (p-p70 S6K), PRAS40 (p-PRAS40), and ribosomal protein S6 (p-S6 235/236) (Figure 4B and Supplemental Figure 2*C*). Interestingly, serum induced increases in p-S6 ribosomal protein was not evident with antibodies recognizing p-S6 240/244. Overall, these data suggest that the mTor pathway is differentially regulated and hyper-responsive in the Traf3ip1^{GT} mutant cells *in vitro* and that Traf3ip1^{GT} mutant cells may have a prolonged response due to impaired down-regulation of the pathway after stimulation.

In contrast to the acetylated microtubule data, our *in vivo* analysis of mTor activity using phospho-S6K levels in Traf3ip1 mutant embryos did not show significant differences compared to the controls (Supplemental Figure 2*D*). This is in agreement with the similar cell size observed *in vivo* in the mutant and control embryos. Taken together, these results suggest that altered mTor signaling may play a role in the increased cell size observed in Traf3ip1^{GT} mutant MEFs and that the effect is a differential response between ciliated and non-ciliated cells in the serum-rich environment of cell culture that may not be present *in vivo*.

The cilium has also been implicated in the normal regulation of several other important signaling pathways, and defects in these pathways help explain several of the phenotypes observed in human ciliopathy patients. In particular, mice with mutations in cilia proteins have defects in Hh signaling (Houde et al., 2006, Haycraft, 2005#172; Huangfu et al., 2003; Liu et al., 2005). Similarly, our analysis of Traf3ip1^{GT} mutant embryos suggest they also have defects related to Hh signaling, as evidenced by polydactyly (as seen in the few embryos that survive to E12.5 and E13.5) as well as abnormalities in neural tube closure and dorsal-ventral patterning. Traf3ip1^{GT} mutant neural tubes showed a loss of Hh expression in the floor plate (Figure 5A, B) and exhibited a dorsalization phenotype. Evaluation of neural tube domains was performed by immunolabeling for the Hh responsive transcription factors Nkx6.1 (Figure 5C, D) and Mnr2 labeling (Figure 5E, F). The Nkx6.1 domain is dramatically diminished while the Mnr2 domain appears to be largely absent. Furthermore, expression of the roof plate marker Msx is expanded ventrally in Traf3ip1^{GT} mutant neural tubes (Figure 5G, H). In order to directly test if Hh signaling is affected in Traf3ip1^{GT} mutants, the Hh reporter mouse line Ptch-lacz was utilized. β-galactosidase staining on whole-mount embryos showed a dramatic reduction in both the neural and endoderm tubes in E10.5 Traf3ip1^{GT} mutant embryos when compared to Traf3ip1^{WT} littermates (Figure 6A–D). Furthermore, sections of caudal neural tube displayed near absence of staining (Figure 6F). Collectively, the localization data, the loss of cilia, and the phenotype of the mutants support a role for Traf3ip1 as a member of the IFT particle (complex B) as has been previously suggested through biochemical analysis in mammalian cells (Follit et al., 2009) and through studies of the homologs in lower eukaryotes (Li et al., 2008).

Activity of the Wnt pathway has also been associated with cilia. Previous data has shown that cilia are important for modulating the balance between canonical and non-canonical Wnt signals and that in the absence of cilia the level of canonical signaling is elevated (for a review see (Gerdes and Katsanis, 2008b)). To assess whether Traf3ip1^{GT} mutant embryos show defects in canonical Wnt signaling, we crossed the Traf3ip1^{GT} mutation onto the

BAT-gal Wnt reporter mouse line (Maretto et al., 2003). Traf3ip1^{GT} mutant embryos did not show overt differences in the BAT-gal reporter expression compared to littermates. One exception was observed in the elevated reporter expression in the brachial arches and eye field compared to controls at embryonic day 10.5 (Figure 7A and B, Supplemental Figure 3A–F; arrows in **B** indicate ectopic Wnt reporter).

The interleukin-13 (IL-13) pathway has been associated with Traf3ip1, where it was identified as a factor interacting with the interleukin-13 receptor alpha 1 (Niu et al., 2003). To investigate whether Traf3ip1 and possibly the cilium are involved in IL-13 signaling activity, Traf3ip1^{GT} mutant and control MEFs were stimulated with IL-13 and the downstream readout of STAT6 phosphorylation was assessed by western blot. The data indicate there are no differences in the resting or stimulated phospho-STAT6 levels between wildtype and Traf3ip1^{GT} mutant cells (Figure 8A). Similarly, whole embryo lysates taken at E10.5 also show no changes in baseline levels of phospho-STAT6 between mutants and wildtypes (Figure 8B). These data suggest that there are no alterations in IL-13 signaling in Traf3ip1^{GT} mutant MEFs and embryos; however, they do not rule out a role for Traf3ip1 in IL-13 signaling in adult tissues.

Discussion

Previous data have indicated that Traf3ip1 is in a complex involved in regulating numerous signaling pathways, such as IL-13 and CD40 (Ling and Goeddel, 2000; Niu et al., 2003). Traf3ip1 mediates its effects on these pathways through interaction with IL-13Rα1 and Traf3 respectively. In previous studies, Traf3ip1 has been shown to inhibit IL-13-induced phosphorylation of STAT6. Traf3ip1 also forms a microtubule attached complex with Traf3 which is released to associate with CD40 receptor upon ligand binding (Ling and Goeddel, 2000; Niu et al., 2003). Traf3ip1 also appears to have a similar function with the protein Disrupted in Schizophrenia 1(DISC1) which associates with microtubules in a Traf3ip1 dependent manner; the significance of the Traf3ip1 interaction with DISC1 is not known (Morris et al., 2003). More recently, data from Traf3ip1 homologs in *C. elegans*, *Chlamydomonas* and Zebrafish suggest that it is important for ciliogenesis as a component of the IFT particle (Kunitomo and Iino, 2008; Li et al., 2008; Omori et al., 2008). Furthermore, support for this possibility was provided by the analyses of ciliary proteomes, by the localization of Traf3ip1 in the cilium of mammalian cells and by immunoprecipitation of Traf3ip1 with complex B IFT proteins (Follit et al., 2009); however, the requirement for Traf3ip1 in mammalian ciliogenesis and its role in mammalian development was not known. We sought to directly address some of these issues using a *Traf3ip1* mutant mouse line to assess whether it has an evolutionarily conserved role in cilia formation and whether it regulates cilia mediated signaling activities.

Indeed, Traf3ip1^{GT} mutant mice are embryonic lethal and phenocopy several other cilia mutants in that they display similar neural tube patterning defects, polydactyly, cardiac edema as well as microphthalmia (Goetz and Anderson, 2010). In addition, cell lines derived from the mutants demonstrate they are unable to form cilia, confirming an evolutionarily conserved function likely as an IFT protein. A role in cilia formation is also supported through analysis of signaling pathways which are impaired due to loss of Traf3ip1. Data

from multiple laboratories have shown that both the Hh and Wnt pathways require the cilium for proper execution of mammalian development (Corbit et al., 2008; Gerdes and Katsanis, 2008a; Gerdes and Katsanis, 2008b; Gerdes et al., 2007; Haycraft et al., 2005; Huangfu et al., 2003; Wiens et al., 2010). Similar to other IFT mutants, Traf3ip1^{GT} mutant mice displayed defects in Hh-dependent dorsal-ventral neural tube patterning and exhibited polydactyly indicative of cilia mediated Hh signaling defects. With regards to canonical Wnt signaling, we detected only subtle changes in spatial BAT-gal reporter gene activity. This result was in direct contrast to data reported in several other studies, but largely agrees with findings by Ocbina *et al*. (Ocbina et al., 2009) analyzing several additional mouse mutants in IFT proteins. Similar subtle changes in the BAT-gal Wnt reporter in cilia mutants have also been recently observed by Lancaster *et al.* (Lancaster et al., 2011) suggesting that cilia mutants in general may have subtle *in vivo* alterations in Wnt activity. It remains to be determined whether the Wnt reporter changes observed in the Traf3ip1 mutant are a direct result of Traf3ip1/cilia loss or secondary to other changes, such as mispositioning of cells. This becomes particularly relevant in the brachial arches in light of the craniofacial and neural crest defects associated with cilia dysfunction (Brugmann et al., 2010; Tobin et al., 2008). Furthermore, the subtle nature of the reporter changes in the Traf3ip1 mutants does suggest that Wnt signaling is largely intact and unperturbed at this embryonic stage of development.

Based on the analyses of the Traf3ip1 homologs in several lower eukaryotic organisms, the inability of Traf3ip1^{GT} mutant mammalian cells to form cilia was not unexpected. However, it was surprising to find that mutant cells displayed a marked increase in cell size, which to our knowledge has not been reported previously as a consequence of cells lacking a cilium. One possible mechanism would be an alteration in mTor activity. The mTor pathway has essential roles in protein translation, proliferation, and is a major influence on cell growth and size regulation. Indeed, our analysis of p70S6K and pS6 (235/236) levels, downstream targets of mTor kinase activity, did confirm increased mTor signaling activity. In fact, Traf3ip1^{GT} mutants appear to display increased and prolonged sensitivity to stimulation compared to controls upon serum addition to the growth medium. This activation could be blocked by rapamycin, an inhibitor of mTor. Although our data do not provide a definitive link between mTor and the increased cell size observed in Traf3ip1^{GT} mutant MEFs, the data indicate that loss of Traf3ip1 alters the strength of the cell's responsiveness to stimuli that activate the mTor pathway. However, we did not observe consistent changes in mTor signaling *in vivo* in Traf3ip1 mutant embryos. This could have been the result of either the cell size phenotype being more subtle *in vivo* and therefore less identifiable, or perhaps the potential for a size change is exacerbated under *in vitro* conditions. Interestingly, it has been suggested that mTor signaling during embryonic development is much more plastic as there appears to be decoupling of some downstream pathways as well as tissue-specific effects [for a review of mTor signaling in development see (Hwang et al., 2008)].

One interesting observation from the mTor data is the differential effect on phosphorylation of S6 ribosomal protein at serine residues 240/244 versus 235/236. The significance of this observation in the cilia mutants remains unknown, but differential phosphorylation has long been observed (Mutoh et al., 1992; Palen and Traugh, 1987). In fact there is evidence to

suggest that S6 kinase is not the only kinase that acts on ribosomal S6 [For a review on S6 ribosomal protein phosphorylation see (Ruvinsky and Meyuhas, 2006)]. There is now even data suggesting that casein kinase 1 may preferentially phosphorylate S6 ribosomal protein at the latter serine residues, particularly serine 247 (Hutchinson et al., 2011). The effects of specific phosphorylation events of S6 ribosomal protein on cell size remain an interesting avenue of investigation. However, it is interesting to note that the knock-in mouse model of a complete phospho-null S6 ribosomal protein leads to a decrease in size in cell types such as MEFs (Ruvinsky et al., 2005).

Defects in normal regulation of mTor could also contribute to some of the phenotypes in human ciliopathy patients. For example, a connection between the cilium and the mTor pathway has been reported for polycystin-1 and tuberous sclerosis-2 (Tsc2). Polycystin-1 is a large ciliary transmembrane protein that interacts with tuberous sclerosis complex, which normally functions to inhibit mTor activity (Dere et al., 2010). Deletion of Tsc2 or polycsytin-1 leads to renal cystic disease that is associated with a marked increase in mTor activity. Interestingly, the renal cystic phenotypes observed in cilia protein mutant models such as the *orpk* (*Ift88*^{Tg737Rpw}) mice and mice lacking the basal body protein Oral-Facial-Digital type I (OFDI) can be greatly diminished by treatment with rapamycin (Zullo et al., 2010).

Another surprising finding in the Traf3ip1^{GT} mutants both *in vitro* and *in vivo* was the increase in the levels of acetylated α-tubulin in the cytosol. Whether this reflects the mislocalization of a modifying enzyme normally resident in the cilium, loss of activity of the deacetylase caused by ciliary defects, or an overall change in microtubule stability is not yet known. Also, it is possible that the loss of Traf3ip1 in mutant cells alters stability of the cytoskeleton that contributes to the changes in cell size observed in culture. Furthermore, it is intriguing that previous data have shown that Traf3ip1 interacts with both actin and tubulin leading to the speculation that Traf3ip1 has a role in cytoskeletal dynamics. Our data indicates that this is likely case as cytoskeletal modifications associated with stabilized microtubules are markedly increased in the Traf3ip1 mutants.

Unlike most cilia proteins, Traf3ip1 was not discovered via analysis of a cilia proteome, a model organism, or ciliopathy patients. Consequently, a body of work regarding Traf3ip1 function existed prior to its identification as a cilia protein. It is feasible that Traf3ip1 mediates its effects on IL-13 and CD40 signaling or DISC1 activity via localization of the receptors and pathway components to the cilium and that these represent novel pathways requiring cilia for normal regulation. Previous localization studies appear to be performed under conditions where cells are not adequately ciliated and thus localization in the cilium could be missed. Although there is a good deal already known about the IFT particle proteins based on studies conducted in lower eukaryotic systems, there is remarkably sparse information about potential cargo transported by the raft, particularly those that associate directly with a known raft component. In addition, it is uncertain as to why there are so many complex B proteins in the IFT particle leading to speculation that particular IFT proteins may be involved in transport of specific cargo. Alternatively, it remains feasible that Traf3ip1 will have additional roles outside of the cilium that involve interactions and sequestration of factors to the cytoskeleton through its microtubule association. With the

generation of this mutant allele it should now be feasible to evaluate some of these possibilities in both *in vivo* and *in vitro* context.

Supplementary Material

Refer to Web version on PubMed Central for supplementary material.

Acknowledgments

This work was supported in part by the National Institutes of Health RO1 (RO1 HD056030) to BKY and (RO1 AI014782), F32 postdoctoral awards (F32 DK088404) to NFB and (F32 AI078662) to NWK, National Polycystic Kidney Foundation Fellowship to NS. We also would like to thank Mandy J. Croyle, Venus Roper and, Jannese Stallworth, Zaki Yazdi and Taylor Kesterson for technical assistance, and Dr. Elizabeth Sztul for the GM130 antibody. Additional support was provided by the UAB Hepatorenal Fibrocystic Diseases Core Center (UAB HRFDCC; NIH P30 DK074038, Dr. Guay-Woodford)

References

Arts HH, Bongers EM, Mans DA, van Beersum SE, Oud MM, Bolat E, Spruijt L, Cornelissen EA, Schuurs-Hoeijmakers JH, de Leeuw N, Cormier-Daire V, Brunner HG, Knoers NV, Roepman R. C14ORF179 encoding IFT43 is mutated in Sensenbrenner syndrome. J Med Genet. 2011; 48:390–5. [PubMed: 21378380]

Berbari NF, Johnson AD, Lewis JS, Askwith CC, Mykytyn K. Identification of Ciliary Localization Sequences within the Third Intracellular Loop of G Protein-coupled Receptors. Mol Biol Cell. 2008; 19:1540–7. [PubMed: 18256283]

Berbari NF, O'Connor AK, Haycraft CJ, Yoder BK. The primary cilium as a complex signaling center. Curr Biol. 2009; 19:R526–35. [PubMed: 19602418]

Boehlke C, Kotsis F, Patel V, Braeg S, Voelker H, Bredt S, Beyer T, Janusch H, Hamann C, Godel M, Muller K, Herbst M, Hornung M, Doerken M, Kottgen M, Nitschke R, Igarashi P, Walz G, Kuehn EW. Primary cilia regulate mTORC1 activity and cell size through Lkb1. Nat Cell Biol. 2010; 12:1115–22. [PubMed: 20972424]

Bonnet CS, Aldred M, von Ruhland C, Harris R, Sandford R, Cheadle JP. Defects in cell polarity underlie TSC and ADPKD-associated cystogenesis. Hum Mol Genet. 2009; 18:2166–76. [PubMed: 19321600]

Brugmann SA, Allen NC, James AW, Mekonnen Z, Madan E, Helms JA. A primary cilia-dependent etiology for midline facial disorders. Hum Mol Genet. 2010; 19:1577–92. [PubMed: 20106874]

Cavalcanti DP, Huber C, Sang KH, Baujat G, Collins F, Delezoide AL, Dagoneau N, Le Merrer M, Martinovic J, Mello MF, Vekemans M, Munnich A, Cormier-Daire V. Mutation in IFT80 in a fetus with the phenotype of Verma-Naumoff provides molecular evidence for Jeune-Verma-Naumoff dysplasia spectrum. J Med Genet. 2011; 48:88–92. [PubMed: 19648123]

Corbit KC, Shyer AE, Dowdle WE, Gaulden J, Singla V, Chen MH, Chuang PT, Reiter JF. Kif3a constrains beta-catenin-dependent Wnt signalling through dual ciliary and non-ciliary mechanisms. Nat Cell Biol. 2008; 10:70–6. [PubMed: 18084282]

Croyle MJ, Lehman JM, O'Connor AK, Wong SY, Malarkey EB, Iribarne D, Dowdle WE, Schoeb TR, Verney ZM, Athar M, Michaud EJ, Reiter JF, Yoder BK. Role of epidermal primary cilia in the homeostasis of skin and hair follicles. Development. 2011; 138:1675–85. [PubMed: 21429982]

Dere R, Wilson PD, Sandford RN, Walker CL. Carboxy terminal tail of polycystin-1 regulates localization of TSC2 to repress mTOR. PLoS One. 2010; 5:e9239. [PubMed: 20169078]

Follit JA, Xu F, Keady BT, Pazour GJ. Characterization of mouse IFT complex B. Cell Motil Cytoskeleton. 2009; 66:457–68. [PubMed: 19253336]

Gerdes JM, Katsanis N. Chapter 7 ciliary function and wnt signal modulation. Curr Top Dev Biol. 2008a; 85:175–95. [PubMed: 19147006]

Gerdes JM, Katsanis N. Ciliary function and Wnt signal modulation. Curr Top Dev Biol. 2008b; 85:175–95. [PubMed: 19147006]

Gerdes JM, Liu Y, Zaghloul NA, Leitch CC, Lawson SS, Kato M, Beachy PA, Beales PL, DeMartino GN, Fisher S, Badano JL, Katsanis N. Disruption of the basal body compromises proteasomal function and perturbs intracellular Wnt response. Nat Genet. 2007; 39:1350–60. [PubMed: 17906624]

Goetz SC, Anderson KV. The primary cilium: a signalling centre during vertebrate development. Nat Rev Genet. 2010; 11:331–44. [PubMed: 20395968]

Goodrich LV, Milenkovic L, Higgins KM, Scott MP. Altered neural cell fates and medulloblastoma in mouse patched mutants. Science. 1997; 277:1109–13. [PubMed: 9262482]

Guo CW, Xiong S, Liu G, Wang YF, He QY, Zhang XE, Zhang ZP, Ge F, Kitazato K. Proteomic analysis reveals novel binding partners of MIP-T3 in human cells. Proteomics. 2010

Hartman TR, Liu D, Zilfou JT, Robb V, Morrison T, Watnick T, Henske EP. The tuberous sclerosis proteins regulate formation of the primary cilium via a rapamycin-insensitive and polycystin 1-independent pathway. Hum Mol Genet. 2009; 18:151–63. [PubMed: 18845692]

Haycraft CJ, Banizs B, Aydin-Son Y, Zhang Q, Michaud EJ, Yoder BK. Gli2 and gli3 localize to cilia and require the intraflagellar transport protein polaris for processing and function. PLoS Genet. 2005; 1:e53. [PubMed: 16254602]

Haycraft CJ, Zhang Q, Song B, Jackson WS, Detloff PJ, Serra R, Yoder BK. Intraflagellar transport is essential for endochondral bone formation. Development. 2007; 134:307–16. [PubMed: 17166921]

Houde C, Dickinson RJ, Houtzager VM, Cullum R, Montpetit R, Metzler M, Simpson EM, Roy S, Hayden MR, Hoodless PA, Nicholson DW. Hippi is essential for node cilia assembly and Sonic hedgehog signaling. Dev Biol. 2006; 300:523–33. [PubMed: 17027958]

Huangfu D, Liu A, Rakeman AS, Murcia NS, Niswander L, Anderson KV. Hedgehog signalling in the mouse requires intraflagellar transport proteins. Nature. 2003; 426:83–7. [PubMed: 14603322]

Hutchinson JA, Shanware NP, Chang H, Tibbetts RS. Regulation of ribosomal protein S6 phosphorylation by casein kinase 1 and protein phosphatase 1. J Biol Chem. 2011; 286:8688–96. [PubMed: 21233202]

Hwang M, Perez CA, Moretti L, Lu B. The mTOR signaling network: insights from its role during embryonic development. Curr Med Chem. 2008; 15:1192–208. [PubMed: 18473813]

Kunitomo H, Iino Y. Caenorhabditis elegans DYF-11, an orthologue of mammalian Traf3ip1/MIP-T3, is required for sensory cilia formation. Genes Cells. 2008; 13:13–25. [PubMed: 18173744]

Lancaster MA, Gopal DJ, Kim J, Saleem SN, Silhavy JL, Louie CM, Thacker BE, Williams Y, Zaki MS, Gleeson JG. Defective Wnt-dependent cerebellar midline fusion in a mouse model of Joubert syndrome. Nat Med. 2011; 17:726–31. [PubMed: 21623382]

Li C, Inglis PN, Leitch CC, Efimenko E, Zaghloul NA, Mok CA, Davis EE, Bialas NJ, Healey MP, Heon E, Zhen M, Swoboda P, Katsanis N, Leroux MR. An essential role for DYF-11/MIP-T3 in assembling functional intraflagellar transport complexes. PLoS Genet. 2008; 4:e1000044. [PubMed: 18369462]

Ling L, Goeddel DV. MIP-T3, a novel protein linking tumor necrosis factor receptor-associated factor 3 to the microtubule network. J Biol Chem. 2000; 275:23852–60. [PubMed: 10791955]

Liu A, Wang B, Niswander LA. Mouse intraflagellar transport proteins regulate both the activator and repressor functions of Gli transcription factors. Development. 2005; 132:3103–11. [PubMed: 15930098]

Maretto S, Cordenonsi M, Dupont S, Braghetta P, Broccoli V, Hassan AB, Volpin D, Bressan GM, Piccolo S. Mapping Wnt/beta-catenin signaling during mouse development and in colorectal tumors. Proc Natl Acad Sci U S A. 2003; 100:3299–304. [PubMed: 12626757]

Morris JA, Kandpal G, Ma L, Austin CP. DISC1 (Disrupted-In-Schizophrenia 1) is a centrosome-associated protein that interacts with MAP1A, MIPT3, ATF4/5 and NUDEL: regulation and loss of interaction with mutation. Hum Mol Genet. 2003; 12:1591–608. [PubMed: 12812986]

Mutoh T, Rudkin BB, Guroff G. Differential responses of the phosphorylation of ribosomal protein S6 to nerve growth factor and epidermal growth factor in PC12 cells. J Neurochem. 1992; 58:175–85. [PubMed: 1309232]

Nauli SM, Alenghat FJ, Luo Y, Williams E, Vassilev P, Li X, Elia AE, Lu W, Brown EM, Quinn SJ, Ingber DE, Zhou J. Polycystins 1 and 2 mediate mechanosensation in the primary cilium of kidney cells. Nat Genet. 2003; 33:129–37. [PubMed: 12514735]

Nauli SM, Kawanabe Y, Kaminski JJ, Pearce WJ, Ingber DE, Zhou J. Endothelial cilia are fluid shear sensors that regulate calcium signaling and nitric oxide production through polycystin-1. Circulation. 2008; 117:1161–71. [PubMed: 18285569]

Niu Y, Murata T, Watanabe K, Kawakami K, Yoshimura A, Inoue J, Puri RK, Kobayashi N. MIP-T3 associates with IL-13Ralpha1 and suppresses STAT6 activation in response to IL-13 stimulation. FEBS Lett. 2003; 550:139–43. [PubMed: 12935900]

Ocbina PJ, Tuson M, Anderson KV. Primary cilia are not required for normal canonical Wnt signaling in the mouse embryo. PLoS One. 2009; 4:e6839. [PubMed: 19718259]

Omori Y, Zhao C, Saras A, Mukhopadhyay S, Kim W, Furukawa T, Sengupta P, Veraksa A, Malicki J. Elipsa is an early determinant of ciliogenesis that links the IFT particle to membrane-associated small GTPase Rab8. Nat Cell Biol. 2008; 10:437–44. [PubMed: 18364699]

Palen E, Traugh JA. Phosphorylation of ribosomal protein S6 by cAMP-dependent protein kinase and mitogen-stimulated S6 kinase differentially alters translation of globin mRNA. J Biol Chem. 1987; 262:3518–23. [PubMed: 3818653]

Pedersen LB, Rosenbaum JL. Chapter Two Intraflagellar Transport (IFT) Role in Ciliary Assembly, Resorption and Signalling. Curr Top Dev Biol. 2008; 85:23–61. [PubMed: 19147001]

Ruvinsky I, Meyuhas O. Ribosomal protein S6 phosphorylation: from protein synthesis to cell size. Trends Biochem Sci. 2006; 31:342–8. [PubMed: 16679021]

Ruvinsky I, Sharon N, Lerer T, Cohen H, Stolovich-Rain M, Nir T, Dor Y, Zisman P, Meyuhas O. Ribosomal protein S6 phosphorylation is a determinant of cell size and glucose homeostasis. Genes Dev. 2005; 19:2199–211. [PubMed: 16166381]

Sharma N, Berbari NF, Yoder BK. Chapter 13 ciliary dysfunction in developmental abnormalities and diseases. Curr Top Dev Biol. 2008; 85:371–427. [PubMed: 19147012]

Tobin JL, Di Franco M, Eichers E, May-Simera H, Garcia M, Yan J, Qu–inlan R, Justice MJ, Hennekam RC, Briscoe J, Tada M, Mayor R, Burns AJ, Lupski JR, Hammond P, Beales PL. Inhibition of neural crest migration underlies craniofacial dysmorphology and Hirschsprung's disease in Bardet-Biedl syndrome. Proc Natl Acad Sci U S A. 2008; 105:6714–9. [PubMed: 18443298]

Wiens CJ, Tong Y, Esmail MA, Oh E, Gerdes JM, Wang J, Tempel W, Rattner JB, Katsanis N, Park HW, Leroux MR. Bardet-Biedl syndrome-associated small GTPase ARL6 (BBS3) functions at or near the ciliary gate and modulates Wnt signaling. J Biol Chem. 2010; 285:16218–30. [PubMed: 20207729]

Zullo A, Iaconis D, Barra A, Cantone A, Messaddeq N, Capasso G, Dolle P, Igarashi P, Franco B. Kidney-specific inactivation of Ofd1 leads to renal cystic disease associated with upregulation of the mTOR pathway. Hum Mol Genet. 2010; 19:2792–803. [PubMed: 20444807]

Research Highlights

- Traf3ip1 plays an evolutionarily conserved role in ciliogenesis
- Traf3ip1 mutant mice display embryonic developmental defects such as neural tube patterning defects, polydactyly, cardiac edema and microphthalmia
- Traf3ip mutant cells display cell size regulation changes associated with altered mTOR signaling
- Mutations in Traf3ip1 lead to altered cilia mediated hedgehog signaling but not to overt changes in canonical Wnt signaling
- Traf3ip1 mutant mice have raised the interesting possibility that cilia may play a role in as yet determined signaling pathways such as IL-13, TNFalpha, or DISC1 biology and cytoskeletal dynamics

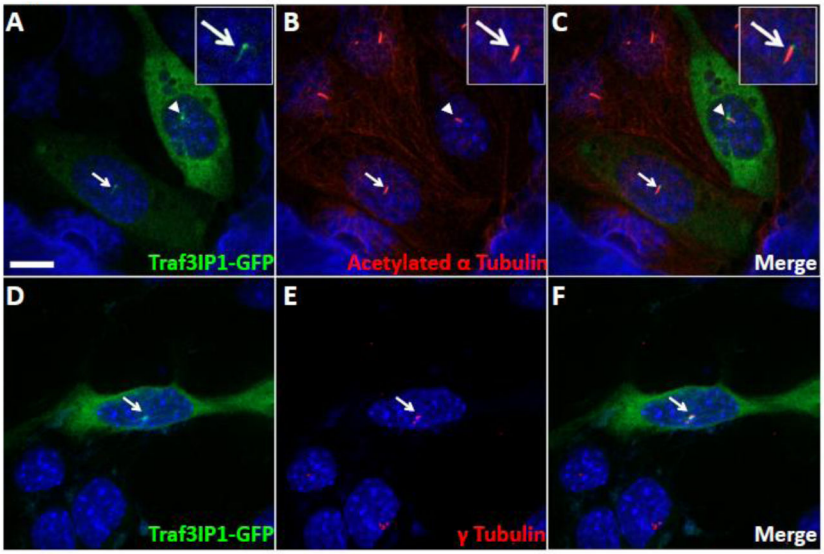

Figure 1. Traf3ip1-GFP expressed in IMCD3 cells localizes to both the cilia axoneme and the basal body

(**A, C**) Traf3ip1-GFP co-localizes with the cilia axoneme (arrows and insets) marker (**B**, **C**) acetylated α-tubulin. (**D**) Traf3ip1-GFP co-localizes with (**E**, **F** arrows) the basal body marker gamma tubulin. Hoescht nuclear label in blue. Scale bar 14 μm.

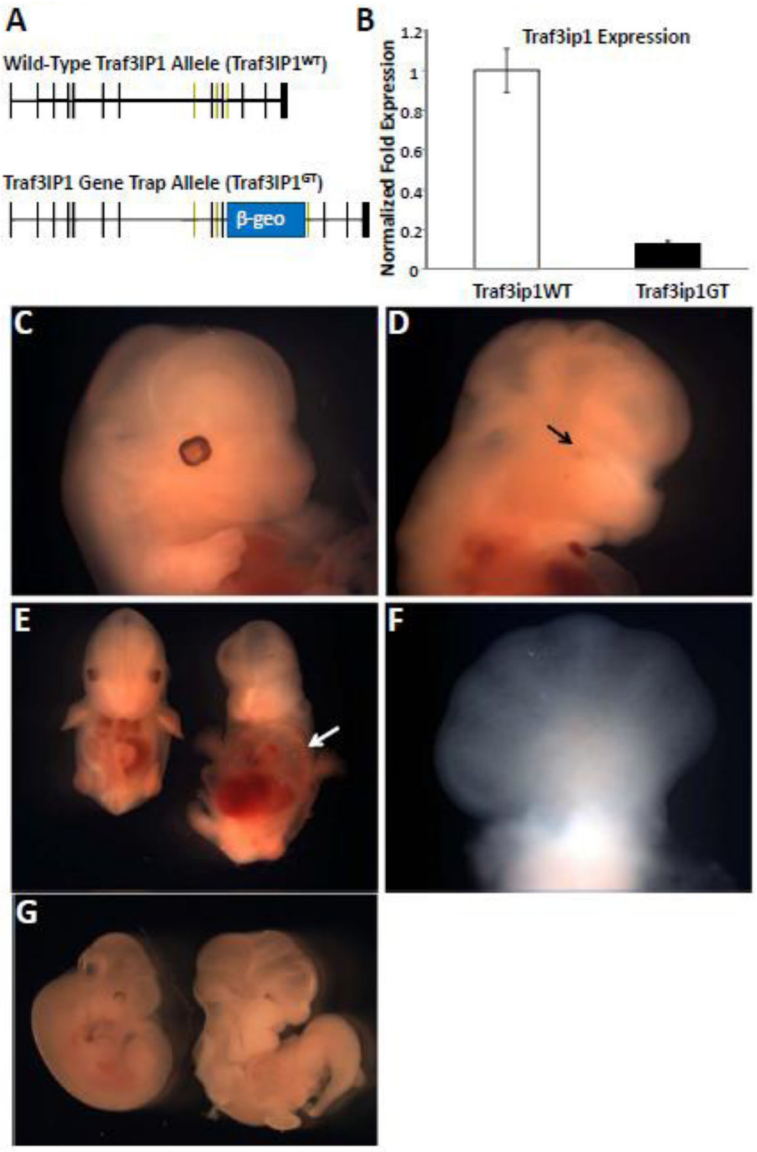

Figure 2. Traf3ip1 mutant mice are embryonic lethal and display phenotypes typically associated with defects in ciliogenesis

(**A**) Schematic of the Traf3ip1 wildtype (Traf3ip1 ^{WT}) and Traf3ip1 mutant gene trap allele (Traf3ip1 ^{GT}). (**B**) Real-time reverse transcriptase PCR results for the expression of Traf3ip1 in homozygous Traf3ip1 ^{WT} and Traf3ip1 ^{GT} mouse embryonic fibroblasts. Expression levels are normalized to the internal control levels of GAPDH and relative to the wildtype level of Traf3ip1. (**C**) The heads of a Traf3ip1 ^{WT} and (**D**) Traf3ip^{GT} mutant embryos at day 10.5 (E10.5) show significant neural developmental defects as well as (**D**, arrow) microphthalmia in the Traf3ip1 ^{GT} mutant. (**E** and **G**) Traf3ip1 ^{WT} embryos on the left and Traf3ip1^{GT} mutant embryos on the right. (**E,** arrow) Significant cardiac edema is observed in the embryonic day 13.5 mutant embryo. (**G**) A curled tail phenotype associated with E10.5 Traf3ip1^{GT} mutant embryos. (**F)** A polydactylous forelimb of an embryonic day 13.5 Traf3ip1 ^{GT} mutant embryo.

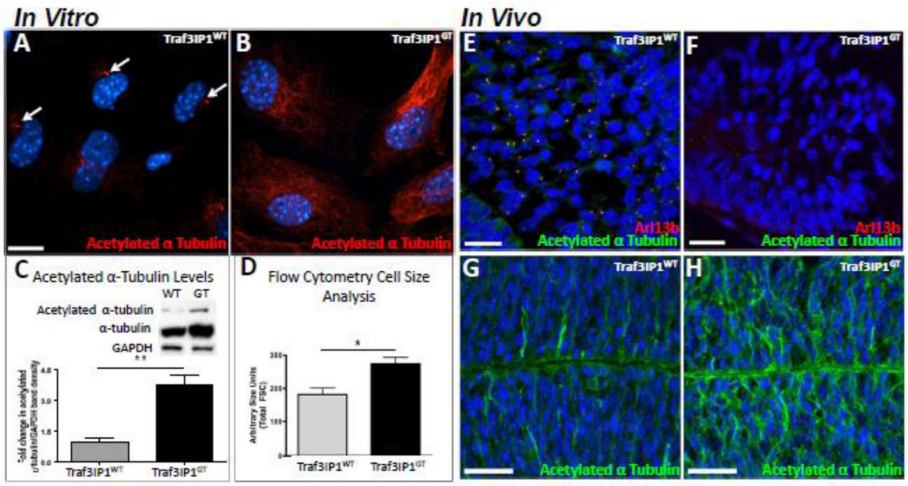

Figure 3. Traf3ip1 cells fail to form cilia both in vitro and in vivo and have elevated levels of acetylated α-tubulin in the cytosol

(**A** and **B**) Traf3ip1 ^{GT} serum starved mouse embryonic fibroblast (MEF) cells in culture fail to form primary cilia as observed by acetylated α-tubulin immunolabeling compared to Traf3ip1^{GT} MEFs. (**B**) Note the marked increase in cell size and acetylated α-tubulin levels in Traf3ip1^{GT} mutants, compared to control cells. (**C**) Total α-tubulin, acetylated α-tubulin, and GAPDH protein levels were determined by western blot and quantitated by densitometry analysis. (**D**) Traf3ip1 ^{WT} and Traf3ip1^{GT} mutant MEF cells were analyzed for cell size/forward scatter (FSC) by flow cytometry. (**E** and **F)** For *in vivo* analysis, E10.5 embryo sections were immunolabeled for the cilia markers Arl13b (red) and acetylated α-tubulin (green) in the lateral plate mesenchyme of a Traf3ip1 ^{WT} embryo while there is a near complete loss in this tissue of the Traf3ip1^{GT} mutants. (**G** and **H**) Embryonic day 10.5 neural tubes were immunolabeled for acetylated α-tubulin in green with Traf3ip1^{WT} and a Traf3ip1^{GT} mutant. Scale bars 14 μm in **A**, **B** and 21μm in **C**, **D** and 43μm in **G**, **H**. Hoescht nuclear label in blue.

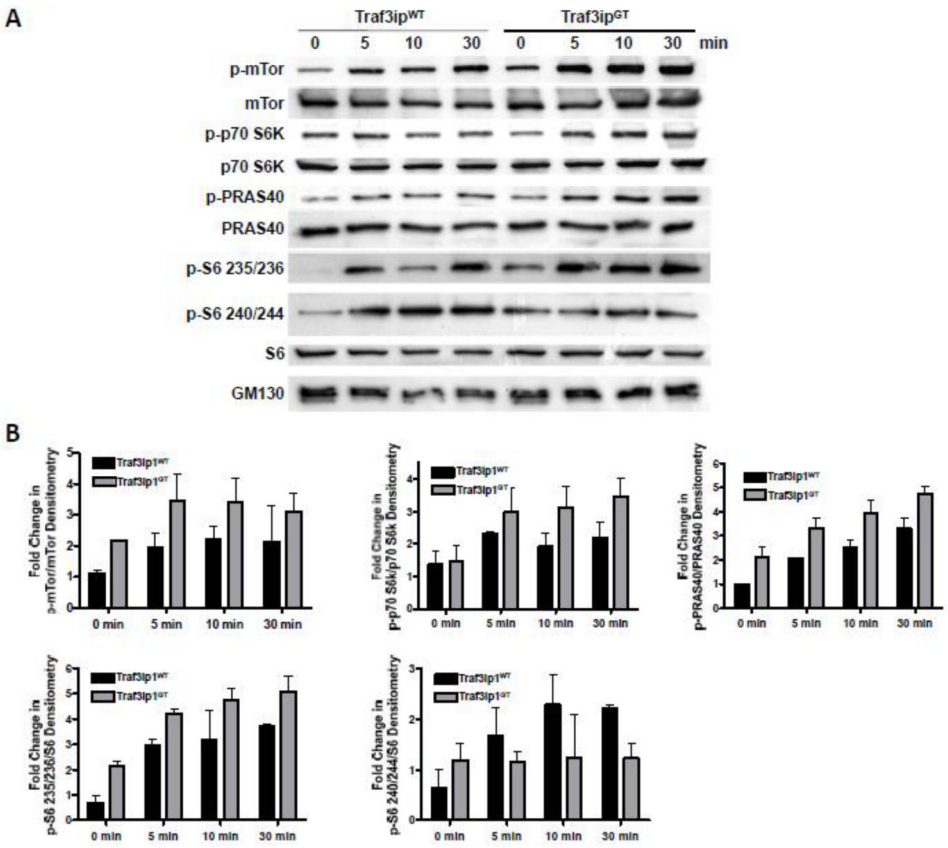

Figure 4. Traf3ip mutant cells display an elevated mTor response to serum

(**A**) Traf3ip1 ^{WT} and Traf3ip1^{GT} mutant MEF cells were cultured for 48 hours with no serum and then exposed to serum for 5, 10, and 30 minutes prior to total protein isolation and western blotting for the following mTor pathway proteins and their phosphorylated forms: phospho-mTor (p-mTor), total mTor (mTor), phospho-p70 S6 kinase (p-p70 S6K), total p70 S6 kinase (p70 S6K), phospho- PRAS40 (p-PRAS40), total PRAS40 (PRAS40), phospho-S6 ribosomal protein serines 235/236 (p-S6 235/236), phospho-S6 ribosomal protein serines 240/244 (p-S6 240/244), total S6 ribosomal protein (S6), and loading control the Golgi marker GM130 (GM130). (**B**) Densitometry analysis of the serum time course, results for fold changes between the total protein and its phosphorylated form(s), are shown for mTor, PRAS40, p70S6 Kinase, S6 ribosomal protein both the serine phosphorylation at sites 235/236 and 240/244.

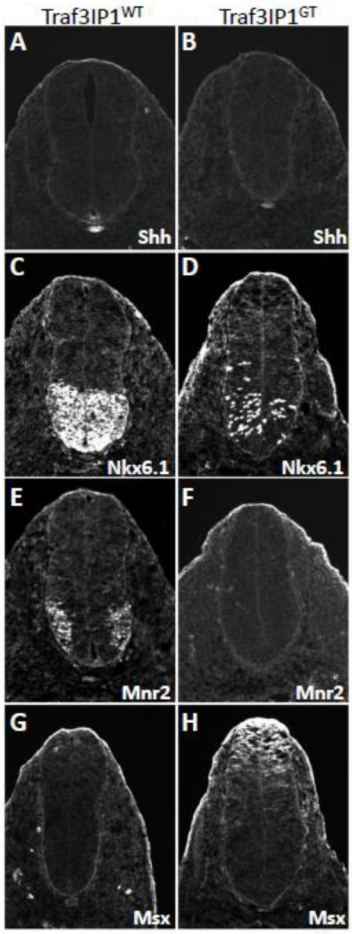

Figure 5. Traf3ip1 mutant embryos have abnormalities in neural tube patterning consistent with defects in cilia mediated Hh signaling

(Left Column) Traf3ip1^{WT} neural tube sections and (Right Column) Traf3ip1^{GT} mutant sections. (**A** and **B**) Sonic Hh labeling of the floor plate is absent in the Traf3ip1^{GT} mutant embryo when compared to its Traf3ip1 ^{WT} littermate. (**D** and **F**) Sonic Hh responsive compartments are either absent or greatly diminished in Traf3ip1^{GT} mutant embryos stained for Nkx6.1 or MNR2 when compared to (**C** and **E**) Traf3ip1 ^{WT} littermates. (**G** and **H**) The roof plate marker MSX is expanded in Traf3ip1^{GT} mutants compared to Traf3ip1^{WT}.

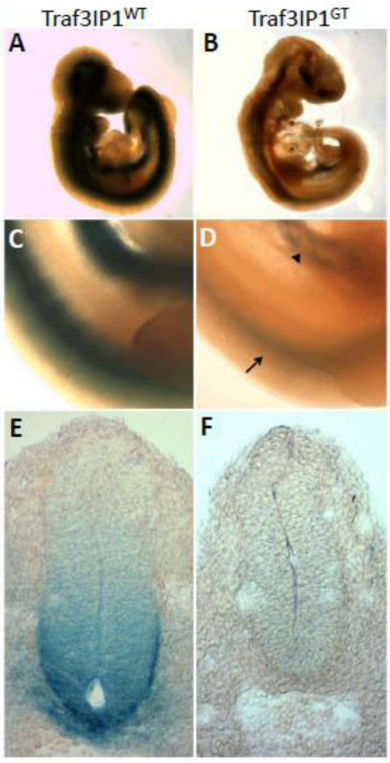

Figure 6. Traf3ip1 mutant embryos display changes in the activity of the Ptch-lacZ Hedgehog reporter

β-galactosidase X-gal staining of Ptch-lacZ Hedgehog reporter mice showed different levels of expression between (**A, C, E**) Traf3ip1 ^{WT} and (**B, D, F**) Traf3ip1^{GT} mutant embryonic day 10.5 embryos. (**B** and **D**) The Traf3ip1^{GT} whole mount mutant embryos show a similar pattern of expression though it is much reduced in both the neural and endoderm tubes (indicated by arrow and arrowhead respectively in panel **D**). (**F**) Also in 60μm thick sections of the caudal neural tube staining is nearly absent in Traf3ip1^{GT} mutant embryos.

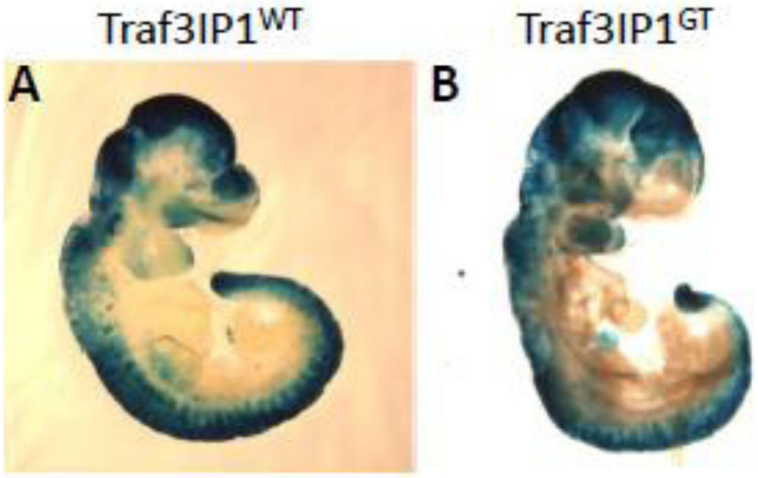

Figure 7. Traf3ip1 mutant embryos do not display major changes in the activity of the BAT-gal Wnt reporter

(**A** and **B**) β-galactosidase X-gal staining of BAT-gal Wnt reporter mice showed similar patterns between Traf3ip1 ^{WT} and Traf3ip1^{GT} mutants embryos at embryonic day 10.5.

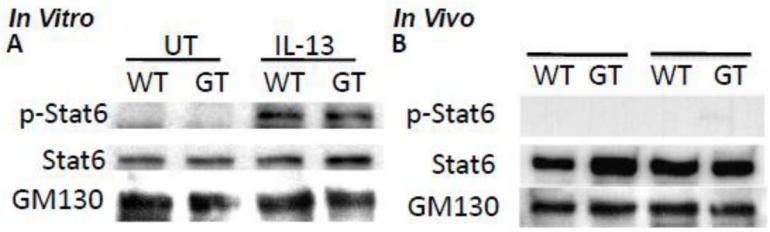

Figure 8. Traf3ip1 mutants do not show changes in IL-13 signaling in vitro or in vivo

(**A**) No changes of the IL-13 downstream response as indicated by phosphorylation of STAT6 in Traf3ip1^{GT} mutant (GT) MEFs treated with recombinant IL-13 compared to wildtype (WT). (**B**) No difference in baseline IL-13 signaling between wildtype (WT) and Traf3ip1^{GT} mutant (GT) E10.5 protein lysates.